TECHNICAL NOTE

A comparative analysis of Acuros XB and the analytical anisotropic algorithm for volumetric modulation arc therapy

Raju P. Srivastava[1, 2], K. Basta[1], Werner De Gersem[2, 3], Carlos De Wagter[2, 3]

[1]Radiotherapy Association Meuse Picardie, Centre Hospitalier Mouscron, Mouscron, Belgium
[2]Department of Radiation Oncology, Ghent University Hospital, Ghent, Belgium
[3]Department of Radiation Oncology and Experimental Cancer Research, Ghent University, Belgium

ABSTRACT

Background: This study aimed to verify the dosimetric impact of Acuros XB (AXB) (AXB, Varian Medical Systems Palo Alto CA, USA), a two model-based algorithm, in comparison with Anisotropic Analytical Algorithm (AAA) calculations for prostate, head and neck and lung cancer treatment by volumetric modulated arc therapy (VMAT), without primary modification to AAA. At present, the well-known and validated AAA algorithm is clinically used in our department for VMAT treatments of different pathologies. AXB could replace it without extra measurements. The treatment result and accuracy of the dose delivered depend on the dose calculation algorithm.

Materials and method: Ninety-five complex VMAT plans for different pathologies were generated using the Eclipse version 15.0.4 treatment planning system (TPS). The dose distributions were calculated using AAA and AXB (dose-to-water, AXB_w and dose-to-medium, AXB_m), with the same plan parameters for all VMAT plans. The dosimetric parameters were calculated for each planning target volume (PTV) and involved organs at risk (OAR). The patient specific quality assurance of all VMAT plans has been verified by Octavius®-4D phantom for different algorithms.

Results: The relative differences among AAA, AXB_w and AXB_m, with respect to prostate, head and neck were less than 1% for PTV $D_{95\%}$. However, PTV $D_{95\%}$ calculated by AAA tended to be overestimated, with a relative dose difference of 3.23% in the case of lung treatment. The absolute mean values of the relative differences were $1.1 \pm 1.2\%$ and $2.0 \pm 1.2\%$, when comparing between AXB_w and AAA, AXB_m and AAA, respectively. The gamma pass rate was observed to exceed 97.4% and 99.4% for the measured and calculated doses in most cases of the volumetric 3D analysis for AAA and AXB_m, respectively.

Conclusion: This study suggests that the dose calculated to medium using AXB_m algorithm is better than AAA and it could be used clinically. Switching the dose calculation algorithm from AAA to AXB does not require extra measurements.

Key words: anisotropic analytical algorithm; planning target volume; volumetric modulated arc therapy; multi-leaf collimator; gamma index

Rep Pract Oncol Radiother 2021;26(3):481–488

Introduction

The Anisotropic Analytical Algorithm has been broadly utilized for dose calculation in the Eclipse treatment planning system. Van Esch et al. [1] reported that AAA improves the accuracy of dose calculations, compared to the single pencil beam (SPB) algorithm, and can achieve 5% agreement with measurements in thoracic phantom. In spite of this, AAA has been noticed to significantly overesti-

Table 1. Number of patients and applied treatment techniques

Pathologies	Number of patients	Treatment techniques
Prostate	35	VMAT
Head and neck	35	VMAT
Lung	25	SBRT

VMAT — volumetric modulated arc therapy; SBRT — stereotactic body radiation therapy

mate the dose near air-tissue interfaces [2]. A novel dose calculation algorithm called Acuros XB, which explicitly solves the Linear Boltzmann Transport Equation (LBTE), has been applied for clinical practice [3]. LBTE is the leading equation that describes the distribution of radiation particles resulting from their interactions with matter. AXB discretizes the space, angle, and energy variables of the LBTE into grids and computes the energy fluence variation of electrons and scattered photons in a substance.

Han et al. [4] and Bush et al. [5] have shown that AXB could reach accuracy comparable to that of Monte Carlo methods, which are broadly considered the gold standard for precise dose calculation used in radiation therapy in phantom experiments, assuming the existence of homogeneous water and heterogeneous media. Several clinical studies have been performed for dosimetric comparison of VMAT and intensity modulated radiation therapy (IMRT) plans between AXB and AAA, indicating that AXB underestimated the doses to PTV or normal tissues in the cases of prostate, lung, head and neck and pelvis treatment, compared to AAA [6–9]. Compared to these results, another study has revealed that AAA underestimated the dose to the spine [7]. The AXB and AAA difference depends on the treatment site and beam energy. AXB provides two dose reporting methods: dose-to-water (AXB_w) and dose-to-medium (AXB_m). For the AXB_w, energy dependent fluence-to-dose response functions are based on water, whereas for the AXB_m they are based on each material. It was a subject of debate whether to select AXB_w or AXB_m for clinical practice [8]. Walters et al. [8] have determined that the dose-to-water method offers a better evaluation of the dose to sensitive tissue in the bone, compared to the dose-to-medium one.

The purpose of this study is to ascertain that implementing the new dose computation algorithm will not majorly change the clinical treatment plans in our department. The study clearly helps new centers that are willing to switch the TPS from AAA to

AXB. The pre-treatment patient-specific quality assurance with the Octavius system will additionally boost up the clinical results.

Materials and methods

Ninety-five patients, who had undergone treatment in our institute during April–December 2019, were included into this study as shown in Table 1.

Dose calculation and planning

For all the three types of pathologies, VMAT plans were generated by the Eclipse TPS for a Clinac iX accelerator, equipped with a Millennium 120 multileaf collimator (MLC) (Varian Medical Systems. Palo Alto. CA. USA), using 6 and 18 MV photon beams. The VMAT plan was created in AXB_m. For the prostate cases, the total dose prescribed to the PTV was 76 Gy, with a daily dose of 2.0 Gy in 38 fractions. The prostate VMAT plans were generated using two full arcs with 6 & 18 MV photon beams, as needed. The head and neck VMAT plans were generated by using two or three full arcs with a 6 MV photon beam and the total prescription dose to PTV was 70 Gy (2.0 Gy/fraction). The prostate and head and neck cases were treated in simultaneous integrated boost (SIB) fractionation schemes. The greatest dose was mentioned for the study. For lung SBRT cases, the prescription dose to PTV was 48 Gy in 4 fractions of 80% of isodose. The VMAT plans for lung SBRT were made using two or three partial arcs with 6 MV photon beam. The dose calculation grid used in this study was 2.5 mm, except for 1.0 mm for lung SBRT cases. Then, each plan was recalculated for AAA and AXB_w, while maintaining the AXB_m calculated monitor units, leaf motion, and beam arrangement. The beam models in AAA and AXB were based on the same physical data.

Evaluation of dosimetric parameters

For the sake of comparison, the relative dose and volume differences in the corresponding dose-vol-

umetric parameters, obtained by AAA and AXB for the same case, were calculated as follows [10]:

$$Relative\ difference\ (\%) = \frac{Value\ of\ AXBx\ -\ Value\ of\ AAA}{Value\ of\ AAA} \times 100$$

where: AXBx is selected between AXB_w and AXB_m depending on what dose reporting mode should be compared.

Evaluation of the plans and statistical analysis

For the PTV, the evaluation parameters included $D_{95\%}$, $D_{98\%}$, minimum dose and the mean dose. For the OARs, the analysis included the mean dose and a set of appropriate V_x values, V_x being the volume of the organ getting a dose of x or more. In the case of OARs, the analysis included an appropriately selected dose or volume parameter. For the rectum and bladder, V30, defined as the volume that receives more than 30 Gy, was analyzed. The absolute doses in this study were presented in Gy and all the numerical data were rounded to the nearest tenth.

Octavius phantom

The 2D-Array, together with Octavius®-4D (PTW-Freiburg, Germany), have been widely described in the literature [11–13]. Figure 1 shows the normal setup of Octavius®-4D with the 2D array detector. An inclinometer mounted on the gantry ensures that the rotation unit always rotates along with the gantry, always keeping the 2D array perpendicular to the beam axis. The beam always hits the detector array in a perpendicular way, because the same face of the detector follows the gantry, so no correction factors are required.

To evaluate the dosimetric agreement between the measured and the calculated dose, the gamma evaluation method, implemented in the Verisoft 7.2.0 version, was used, where the measured dose matrix was used as reference. This calculation of the gamma index is based on the concept Low [14]. A two-sample paired t-test was used to compare the results for the average dose $D_{95\%}$, $D_{98\%}$ and D_{max} of PTV prostate, head and neck and lung pathologies. A p-value < 0.05 was considered statistically significant.

Results

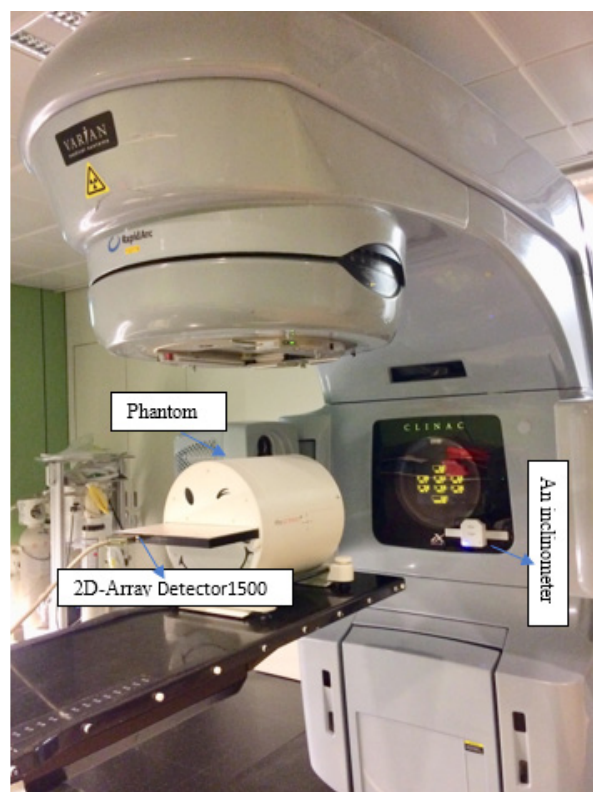The relative differences among AAA, AXB_w and AXB_m, with respect to prostate, head and neck and

Figure 1. Standard setup of Octavius® 4D system in measurement position with Detector 1500 inserted in a cylindrical phantom that rotates synchronously with the gantry and the inclinometer attached to the gantry

lung cases, are shown in Figure 2. The PTV $D_{95\%}$ and $D_{98\%}$ were within 1.0 ± 0.23% difference between AXB_w and AXB_m to the AAA algorithm, for the prostate and head and neck cases, however, the value increases up to 3.23 ± 0.26% for the lung cases treatment by SBRT. Bladder V_{30} shows 1.3 ± 0.31% and 2.6 ± 0.29% difference between AAA and AXB_w, AXB_m, respectively. The maximum difference was found to be 4% for esophagus mean dose and 2.12% in D_{max} spinal cord in the treatment of head and neck pathologies. The maximum dose to the thoracic wall was underestimated with maximum value of the relative dose difference of 3.95% from AAA during the treatment of SBRT.

Several factors may explain the fact that no significant dose differences were found at the level of the spinal cord. Unlike the lungs, the spinal cord receives most of its dose by scatter. Additionally, the much lower density of the lungs, compared to water, can easily result in higher difference in different dose calculation algorithms because of increased electron interaction paths. Whether dose computation algorithms compute significantly different
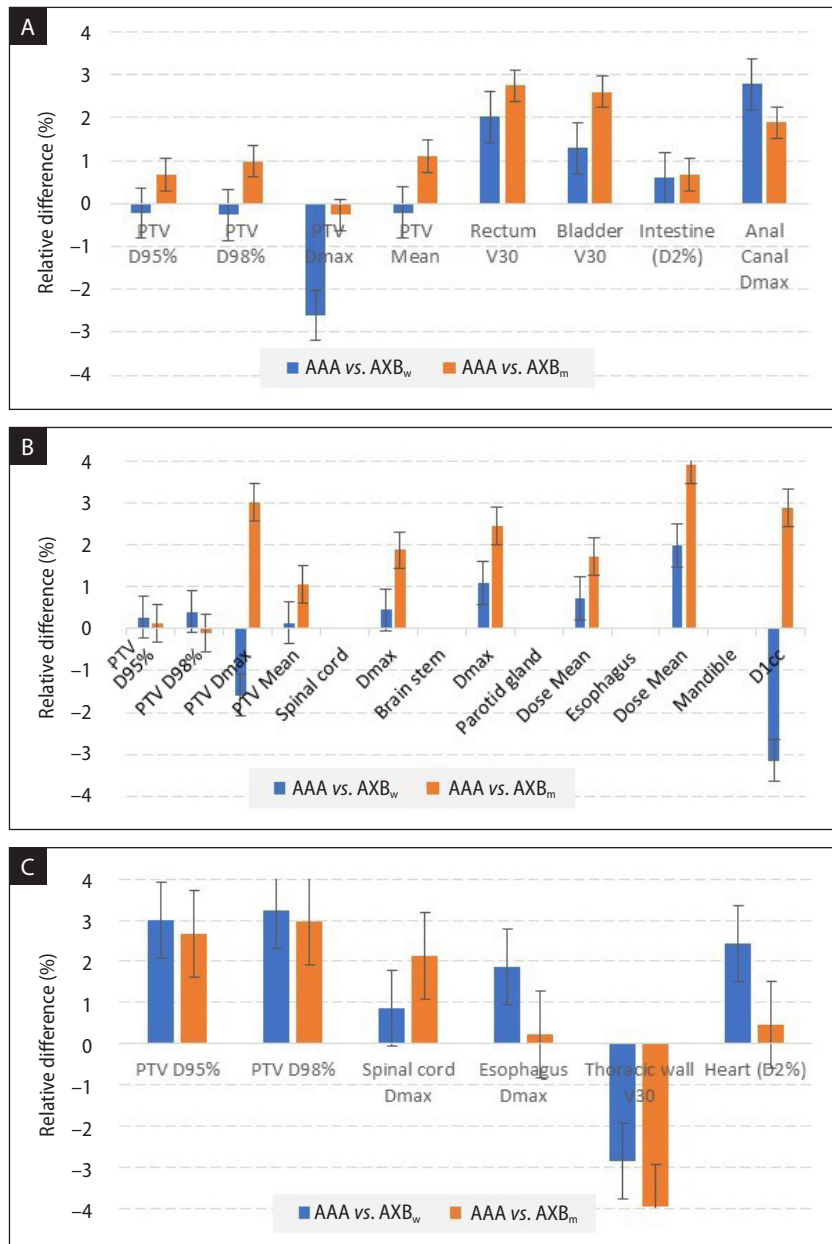
Figure 2. The relative difference for planning target volume (PTV) and organ at risk for (**A**) prostate; (**B**) head and neck; (**C**) lung cases. Statistical error indicates standard error

doses in lower or higher density regions depends on the fine details of the dose computation methods, such as scaling of the pre-computed Monte Carlo kernels with respect to density.

The average dose $D_{95\%}$, $D_{98\%}$ and D_{max} of PTV with respect to prostate, head and neck and lung cases for AAA, AXB_w, and AXB_m are shown in Table 2. The p-value has been calculated for the average dose $D_{95\%}$, $D_{98\%}$ and D_{max} of PTV between AAA, AXB_w, and AXB_m. These results were found significant (p < 0.05) for AAA and AXB to all pathologies.

All the plans were analyzed [14] and the γ-pass rate with the 3% dose tolerance and 3 mm distance was calculated to harmonize the relation to the treatment planning system. Table 3 summarizes the results of the average g-passing rate for the different pathologies examined in the present study, by 2D and 3D analysis for AAA, AXBw and AXBm. The results demonstrated that the gamma pass rates for all the plans were higher than ≤ 97.0 % by volumetric 3D analysis, where a 10% low-dose threshold was fixed [15]. Our clini-

Table 2. The planning target volume (PTV) dose ($D_{95\%}$, $D_{98\%}$ and D_{max}) for prostate, head and neck and lung cases. Statistical error indicates standard deviation. p_{A-m}: p-value between AAA and AXB_m. p_{A-w}: p-value between AAA and AXB_w

PTV	AAA	AXB_m	AXB_w	pA-m	pA-w
Prostate					
$D_{95\%}$	75 .53 ± 0 .6	74 .69 ± 0 .4	74 .96 ± 0 .3	0.01	0.006
$D_{98\%}$	74 .28 ± 0 .5	73 .89 ± 0 .3	74 .68 ± 0 .3	0.02	0.004
D_{max}	79.43 ± 0 .4	78.25 ± 0 .4	80.59 ± 0 .6	0.01	0.001
Head and neck					
$D_{95\%}$	68 .97 ± 0 .8	68 .58 ± 0 .6	68 .88 ± 0 .6	0.037	0.026
$D_{98\%}$	68 .52 ± 0 .6	68 .59 ± 0 .3	68 .64 ± 0 .8	0.022	0.005
D_{max}	74 .84 ± 1 .2	73 .86 ± 0 .9	74 .59 ± 1 .0	0.031	0.007
Lung					
$D_{95\%}$	50 .01 ± 0 .9	48 .68 ± 0 .5	48 .51 ± 0 .4	0.04	0.06
$D_{98\%}$	48 .37 ± 1 .1	46 .93 ± 0 .8	46 .81 ± 0 .6	0.02	0.05
D_{max}	60 .21 ± 0 .4	60 .12 ± 0 .5	60 .06 ± 0 .5	0.01	0.02

Table 3. Average γ-passing rates for AAA, AXB_w and AXB_m for different pathologies in planar 2D and volumetric 3D analysis. Statistical error indicates standard deviation

Pathologies	Planar analysis			Volumetric 3D analysis
	2D			
	Coronal	Sagittal	Transversal	
Gamma passing rates (%) for AAA				
Prostate	95.8 ± 1.7	96.5 ± 0.2	96.2 ± 0.4	97.9 ± 1.2
Head and neck	97.2 ± 0.3	97.3 ± 1.1	98.1 ± 0.8	98.1 ± 1.1
Lung	91.8 ± 1.9	91.2 ± 0.5	94.7 ± 1.1	97.4 ± 1.4
Gamma passing rates (%) for AXBw				
Prostate	96.6 ± 0.3	95.8 ± 1.1	96.2 ± 0.6	97.5 ± 0.4
Head and neck	96.2 ± 0.3	96.9 ± 0.5	98.2 ± 0.5	98.7 ± 0.5
Lung	99.1 ± 0.1	99.2 ± 0.3	99.6 ± 0.1	99.7 ± 0.3
Gamma passing rates (%) for AXBm				
Prostate	96.8 ± 1.5	96.5 ± 1.3	97.4 ± 0.8	99.4 ± 0.6
Head and neck	97.4 ± 1.4	97.8 ± 1.5	97.6 ± 1.0	99.6 ± 0.3
Lung	95.8 ± 1.1	95.1 ± 1.1	99.6 ± 0.3	99.7 ± 0.1

cal standard of 95% or greater for the gamma index percentage was standardized and was achieved for all the plans.

Discussion

For many years, the methods used to inter-compare the calculated doses to be delivered to different media have been subject to scientific debate [8]. This debate has generally addressed what is the best quantity to score (dose to medium or dose to water) with respect to the biological effect of radiation.

Table 4 shows an overview of literature comparisons to the study.

Rana et al. [6] used Rapid Arc plans to perform a planning study of prostate cancer patients in which the clinical dosimetric effects of AAA and AXB were compared. Our results confirm their findings (range –0.21–0.67%) concerning the PTV $D_{95\%}$.

Kan et al. [16] reported that the mean and minimum doses to the PTV_{70} calculated by AXB were reduced by AAA for nasopharyngeal carcinoma. They found –2.0% and 4.0% discrepancies for

Table 4. An overview of literature comparisons to current study

Literature data	Pathologies	Treatment technique	AAA *vs.* AXB$_m$	Current study	
				AAA *vs.* AXB$_m$	AAA *vs.* AXB$_w$
Fogliata A et al. 2012	Lung	VMAT	< 0.5%	2.6%	3.0%
Rana S et al. 2013	Prostate	VMAT	0.5%	0.67%	-0.21%
Kan MW et al. 2013	Head and neck	VMAT	−2.0%	0.14%	1.01%
Han T et al. 2013	Lung phantom	IMRT and VMAT	−2.2%	2.6%	3.0%
Lui et al. 2014	Lung	SBRT	−2.1%	2.6%	3.0%
Hirata K et al. 2015	Head and neck	VMAT	2.6%	0.14%	1.01%
Kumar L et al. 2020	Breast	Breath hold	1.0%	NA	NA
Bassi S et al. 2020	Phantom study	Static	1.8%	NA	NA

VMAT — volumetric modulated arc therapy; IMRT — intensity modulated radiation therapy; SBRT — stereotactic body radiation therapy; NA — not applicable

AXB$_m$ and AXB$_w$ in bone content. The results of the current study showed that AAA computed, on average, an up to 1.01% higher maximum PTV dose than AXB$_m$, which was used for generating the treatment plans. Hirata et al. [17] determined that AXB showed agreement with the measurements within 2.6% at the high-density area, while AAA and PBC calculations overestimated the dose by more than 4.5% and 4.0%, respectively. These findings are in agreement to those of Fogliata et al. [18]. They showed the difference in the doses calculated using AXB and AAA was within 3% in lung planning target volumes. Bassi et al. [19] validated AXB in the presence of inhomogeneities for VMAT. They reported up to 1.8% dose calculated uncertainties with AXB. The absolute dose measured with Gaf-Chromic EBT in the heterogeneous phantom in the abdominal region proved that the dose differences after the air calculated by AXB are less than 3% while with AAA differences up to 11% can be obtained. Soh et al. [20] displayed ± 1.5% difference between AAA and AXB algorithm predicted depth dose, excluding the surface and buildup doses.

Han et al. [4] reported that AAA and AXB dose calculations agreed well with RPC lung phantom to TLD and film measurements for IMRT and VMAT plans. The cause for this small difference between AXB and AAA is attributed to the modeling of the heterogeneity of lung tissue in the AXB, compared to AAA, as reported by other studies [21]. Robinson D [22] has demonstrated that AAA overestimates the doses to the heterogeneity interface. Supporting this finding, Liu et al. [23] have also reported lower conformity (−2.1%), compared to AAA. Tajaldeen et al. [24] showed 2.3%, 1.3% and 0.7% discrepancies between AAA, AXB$_w$ and AXB$_m$

algorithms and measured dose, respectively. Kumar et al. [25] found less than 1% discrepancy between AAA and AXB for mean PTV dose in deep-inspiration breath-hold respiratory techniques used for the treatment of left breast cancer.

In 2002, Liu [8] asserted that the dose-to-medium method allows a closer relationship between tissue response and dose, while Keall Paul argued against this statement and specified that all clinical knowledge and dosimetry protocols are based on the dose-to-water mode.

Eclipse AXB is based on the macroscopic cross sections of the media assigned from the CT scan for transport of photons and electrons. A biological material, such as the lung, adipose tissue, muscle, cartilage, or bone, can be assigned for voxels with a density < 3 g/cm^3. The voxels are assigned a material design corresponding to the weighted proportion of the materials, when the density ranges overlap (e.g., adipose and muscle). AXB$_m$ used the energy deposition cross section or restricted electronic stopping power from the medium at that point. AXB$_m$ is then intrinsically computed so that the TPS reference dose should be specified in water, because the difference between water and tissue is inherently captured [26].

The results emphasize that several factors affect plan evaluation when using the Octavius®-4D phantom. They are especially improved if the more limiting local γ-index computation approach is used. Indeed, the global γ-index produces more homogeneous results with higher passing rates, because its tolerance level is computed with respect to the value of the maximum dose. The 2D approach considers each slice as independent of the surrounding volume, with the drawback that the

results are strongly dependent on the chosen plane, without a certain significant correlation between the magnitude of errors of different plans [27]. The 3D analysis allows a slice-by-slice evaluation, also considering the neighboring slices. Our results confirmed that the single slice evaluation (2D) always had an inferior agreement, compared to the 3D analysis and volumetric γ-index. Pulliam et al. [28] compared the two gamma results, using Monte Carlo computation as reference dose distribution, and quantified the increase of the passing pixels percent up to 3.2% in the 3D analysis, confirming our findings. Moreover, some problems that would be identified with 3D analysis might be missed in 2D individual planes. The 3D analysis could also highlight local regions where problems exist.

Conclusion

In the present study, the results showed that doses calculated to medium by AXB_m could be used clinically for VMAT application. Moving from AAA to AXB does not require extra measurements because the dose difference between AAA and AXB were small in prostate and head and neck pathologies. However, the appropriateness of switching the dose calculation algorithm from AAA to AXB should be confirmed carefully from a clinical viewpoint in lung pathologies. AXB_m results in advantage not only for prostate and head and neck but also for lung pathologies over AAA.

Conflict of interest

Funding

References

1. Van Esch A, Tillikainen L, Pyykkonen J, et al. Testing of the analytical anisotropic algorithm for photon dose calculation. Med Phys. 2006; 33(11): 4130–4148, doi: 10.1118/1.2358333, indexed in Pubmed: 17153392.
2. Fogliata A, Nicolini G, Clivio A, et al. Dosimetric validation of the anisotropic analytical algorithm for photon dose calculation: fundamental characterization in water. Phys Med Biol. 2006; 51(6): 1421–1438, doi: 10.1088/0031-9155/51/6/004, indexed in Pubmed: 16510953.
3. Vassiliev ON, Wareing TA, McGhee J, et al. Validation of a new grid-based Boltzmann equation solver for dose calculation in radiotherapy with photon beams. Phys Med Biol. 2010; 55(3): 581–598, doi: 10.1088/0031-9155/55/3/002, indexed in Pubmed: 20057008.
4. Han T, Followill D, Mikell J, et al. Dosimetric impact of Acuros XB deterministic radiation transport algorithm for heterogeneous dose calculation in lung cancer. Med Phys. 2013; 40(5): 051710, doi: 10.1118/1.4802216, indexed in Pubmed: 23635258.
5. Bush K, Gagne IM, Zavgorodni S, et al. Dosimetric validation of Acuros XB with Monte Carlo methods for photon dose calculations. Med Phys. 2011; 38(4): 2208–2221, doi: 10.1118/1.3567146, indexed in Pubmed: 21626955.
6. Rana S, Rogers K, Lee T, et al. Dosimetric impact of Acuros XB dose calculation algorithm in prostate cancer treatment using RapidArc. J Cancer Res Ther. 2013; 9(3): 430–435, doi: 10.4103/0973-1482.119328, indexed in Pubmed: 24125978.
7. Huang B, Wu L, Lin P, et al. Dose calculation of Acuros XB and Anisotropic Analytical Algorithm in lung stereotactic body radiotherapy treatment with flattening filter free beams and the potential role of calculation grid size. Radiat Oncol. 2015; 10: 53, doi: 10.1186/s13014-015-0357-0, indexed in Pubmed: 25886628.
8. Liu HH. Dm rather than Dw should be used in Monte Carlo treatment planning. For the proposition. Med Phys. 2002; 29(5): 922–923, doi: 10.1118/1.1473137, indexed in Pubmed: 12033589.
9. Walters BRB, Kramer R, Kawrakow I. Dose to medium versus dose to water as an estimator of dose to sensitive skeletal tissue. Phys Med Biol. 2010; 55(16): 4535–4546, doi: 10.1088/0031-9155/55/16/S08, indexed in Pubmed: 20668336.
10. Zhen H, Hrycushko B, Lee H, et al. Dosimetric comparison of Acuros XB with collapsed cone convolution/superposition and anisotropic analytic algorithm for stereotactic ablative radiotherapy of thoracic spinal metastases. J Appl Clin Med Phys. 2015; 16(4): 181–192, doi: 10.1120/jacmp.v16i4.5493, indexed in Pubmed: 26219014.
11. Allgaier B, Schüle E, Würfel J. Dose reconstruction in the OCTAVIUS 4D phantom and in the patient without using dose information from the TPS. White Paper PTW, Freiburg 2013.
12. Stathakis S, Myers P, Esquivel C, et al. Characterization of a novel 2D array dosimeter for patient-specific quality assurance with volumetric arc therapy. Med Phys. 2013; 40(7): 071731, doi: 10.1118/1.4812415, indexed in Pubmed: 23822435.
13. Van Esch A, Basta K, Evrard M, et al. The Octavius1500 2D ion chamber array and its associated phantoms: dosimetric characterization of a new prototype. Med Phys. 2014; 41(9): 091708, doi: 10.1118/1.4892178, indexed in Pubmed: 25186383.
14. Low DA, Harms WB, Mutic S, et al. A technique for the quantitative evaluation of dose distributions. Med Phys. 1998; 25(5): 656–661, doi: 10.1118/1.598248, indexed in Pubmed: 9608475.
15. Nelms BE, Simon JA. A survey on planar IMRT QA analysis. J Appl Clin Med Phys. 2007; 8(3): 76–90, doi: 10.1120/jacmp.v8i3.2448, indexed in Pubmed: 17712302.
16. Kan MWK, Leung LHT, Yu PKN. Dosimetric impact of using the Acuros XB algorithm for intensity modulated radiation therapy and RapidArc planning in nasopharyngeal carcinomas. Int J Radiat Oncol Biol Phys. 2013; 85(1):

e73–e80, doi: 10.1016/j.ijrobp.2012.08.031, indexed in Pubmed: 23040220.

17. Hirata K, Nakamura M, Yoshimura M, et al. Dosimetric evaluation of the Acuros XB algorithm for a 4 MV photon beam in head and neck intensity-modulated radiation therapy. J Appl Clin Med Phys. 2015; 16(4): 52–64, doi: 10.1120/jacmp.v16i4.5222, indexed in Pubmed: 26218997.

18. Fogliata A, Nicolini G, Clivio A, et al. Critical appraisal of Acuros XB and Anisotropic Analytic Algorithm dose calculation in advanced non-small-cell lung cancer treatments. Int J Radiat Oncol Biol Phys. 2012; 83(5): 1587–1595, doi: 10.1016/j.ijrobp.2011.10.078, indexed in Pubmed: 22300575.

19. Bassi S, Tyner E. 6X acuros algorithm validation in the presence of inhomogeneities for VMAT treatment planning. Rep Pract Oncol Radiother. 2020; 25(4): 539–547, doi: 10.1016/j.rpor.2020.03.018, indexed in Pubmed: 32494226.

20. Soh RC, Tay GH, Lew WS, et al. A depth dose study between AAA and AXB algorithm against Monte Carlo simulation using AIP CT of a 4D dataset from a moving phantom. Rep Pract Oncol Radiother. 2018; 23(5): 413–424, doi: 10.1016/j.rpor.2018.08.003, indexed in Pubmed: 30197577.

21. Fogliata A, Nicolini G, Clivio A, et al. Dosimetric evaluation of Acuros XB Advanced Dose Calculation algorithm in heterogeneous media. Radiat Oncol. 2011; 6: 82, doi: 10.1186/1748-717X-6-82, indexed in Pubmed: 21771317.

22. Robinson D. Inhomogeneity correction and the analytic anisotropic algorithm. J Appl Clin Med Phys. 2008; 9(2): 112–122, doi: 10.1120/jacmp.v9i2.2786, indexed in Pubmed: 18714283.

23. Liu HW, Nugent Z, Clayton R, et al. Clinical impact of using the deterministic patient dose calculation algorithm Acuros XB for lung stereotactic body radiation therapy. Acta Oncol. 2014; 53(3): 324–329, doi: 10.3109/0284186X.2013.822552, indexed in Pubmed: 23957683.

24. Tajaldeen A, Ramachandran P, Alghamdi S, et al. On the use of AAA and AcurosXB algorithms for three different stereotactic ablative body radiotherapy (SABR) techniques: Volumetric modulated arc therapy (VMAT), intensity modulated radiation therapy (IMRT) and 3D conformal radiotherapy (3D-CRT). Rep Pract Oncol Radiother. 2019; 24(4): 399–408, doi: 10.1016/j.rpor.2019.02.008, indexed in Pubmed: 31333334.

25. Kumar L, Kishore V, Bhushan M, et al. Impact of acuros XB algorithm in deep-inspiration breath-hold (DIBH) respiratory techniques used for the treatment of left breast cancer. Rep Pract Oncol Radiother. 2020; 25(4): 507–514, doi: 10.1016/j.rpor.2020.04.011, indexed in Pubmed: 32494224.

26. Kry SF, Feygelman V, Balter P, et al. AAPM Task Group 329: Reference dose specification for dose calculations: Dose-to-water or dose-to-muscle? Med Phys. 2020; 47(3): e52–e64, doi: 10.1002/mp.13995, indexed in Pubmed: 31883390.

27. Budgell GJ, Perrin BA, Mott JHL, et al. Quantitative analysis of patient-specific dosimetric IMRT verification. Phys Med Biol. 2005; 50(1): 103–119, doi: 10.1088/0031-9155/50/1/009, indexed in Pubmed: 15715426.

28. Pulliam KB, Huang JY, Howell RM, et al. Comparison of 2D and 3D gamma analyses. Med Phys. 2014; 41(2): 021710, doi: 10.1118/1.4860195, indexed in Pubmed: 24506601.